Channel, Doppler Frequency Shift, and Velocity Estimation in UAV Systems with mmWave Communication Links

Abhishek Agrahari, Mandar R. Nalavade, and Gaurav S. Kasbekar

***Abstract*—We address the problem of accurately estimating the channel and the Doppler frequency shift between an Unmanned Aerial Vehicle (UAV) and a Ground Station (GS), and hence the velocity of the UAV, when they communicate using antenna arrays and millimeter wave (mmWave) bands. This estimation process is useful since it leads to higher data rates of the communication link between the UAV and the GS through the adaptation of the modulation and coding scheme and optimization of the antenna array parameters. It also enables the adjustment of the carrier frequency to optimize the communication, tracking of the motion of the UAV and planning of its future trajectory, etc. Estimation schemes proposed in prior work suffer from various limitations such as inapplicability to non-linear channel models, large estimation errors, etc. We propose an improved scheme for estimating the UAV channel, Doppler frequency shift, and velocity. Our technique is based on maximum likelihood estimation (MLE) of the parameters of the UAV and the GS in the beam-space. Using extensive numerical computations, we show that our proposed scheme computes estimates of the channel, Doppler frequency shift, as well as UAV velocity that are highly accurate; also, the mean errors of the estimates of the Doppler frequency shift computed by our proposed scheme are much closer to zero than those of the estimates computed using the state-of-the-art chirplet transform based algorithm.**

***Index Terms*—Unmanned Aerial Vehicle (UAV), Beam-steering, Maximum Likelihood Estimation, Channel Information, Doppler Frequency Shift, Millimeter Wave Communication**

I. Introduction

Unmanned Aerial Vehicles (UAVs) have numerous military as well as civilian applications such as search and rescue missions, precision agriculture, remote sensing, border surveillance, traffic monitoring, aerial photography, environmental monitoring, etc. [1]. UAV communication, including the communication between a UAV and a ground station (GS) and that between different UAVs, needs to be effectively performed in order to ensure the proper operation of UAV missions [1]. The use of millimeter wave (mmWave) frequencies in UAV communication has the potential to provide high data rates due to the large amount of free bandwidth available in mmWave bands, highly focused communication, and the use of multiple concurrent communication links. Further, the short wavelengths of mmWave bands allow the use of compact antenna arrays. These are advantageous since they enable the deployment of directional communication, precoding, and coherent combining techniques [2]. However, mmWave communication also poses several challenges such as susceptibility to high path loss, obstacles, and blockages, which can be mitigated through advanced beam-steering techniques [3], [4]. These adaptive approaches adjust the beam direction in real-time based on the location of the UAV.

The UAV's motion can lead to signal attenuation and potential disruptions in communications. Also, in UAV communication, the relative motion between the transmitter and receiver leads to a shift in perceived frequency, which is known as Doppler frequency shift [5]. The perceived frequency shoots up or down depending on whether the distance between the transmitter and receiver decreases or increases. Hence, channel estimation accuracy may also be compromised [6]. The objective of this paper is to accurately estimate the channel and the Doppler frequency shift between a UAV and a GS, and hence the velocity of the UAV, when they communicate using antenna arrays and mmWave bands. This estimation process is useful since it leads to enhanced performance (e.g., higher data rates) of the communication link between the UAV and the GS as the estimated UAV parameters can be used to determine the transmission scheme and parameters. The modulation and coding scheme can be adapted to the computed estimate of the UAV channel, and the antenna array parameters can be optimized for effective transmission based on the knowledge of the channel. Also, the Doppler frequency shift estimate can be used for adjusting the carrier frequency to optimize the communication between the UAV and the GS. Finally, the computed UAV velocity estimate can be used for tracking the motion of the UAV, planning its future trajectory.

Schemes proposed in prior work for the estimation of the UAV channel, Doppler frequency shift, and velocity (see Section II for a review) suffer from various limitations such as inapplicability to non-linear channel models, large estimation errors, etc. Motivated by the need to address the above limitations of prior work, the main contributions of this paper are summarized as follows. We propose an improved scheme for estimating the UAV channel, Doppler frequency shift, and velocity, when it communicates with a GS using antenna arrays and mmWave frequency bands. We have employed digital antenna array steering for novel beamforming based on relative phase computation. Further, we have derived expressions for a composite beam output and channel estimator between the UAV and the GS. Our technique is based on the maximum likelihood estimation (MLE) of the parameters of the UAV and the GS in the beam-space. Beam-steering proposed in this work refers to the process of electronically adjusting the direction of a beam of electromagnetic waves towards the UAV from the elements of a Uniform Planar Array (UPA) at the GS. The antenna array output can be pointed in a particular direction by adding appropriate phase shifts to each element. MmWave bands offer wide bandwidths, which is beneficial for quantifying changes in the frequency due to Doppler shifts. Further, they allow a high-resolution estimation of the UAV's

The authors are with the Department of Electrical Engineering, Indian Institute of Technology (IIT) Bombay, Mumbai, 400076, India. Their email addresses are abhishekagrahari@gmail.com, 22d0531@iitb.ac.in, and gskasbekar@ee.iitb.ac.in. The work of A. Agrahari and G.S. Kasbekar has been supported in part by the project with code RGSTC01-001. The work of M.R. Nalavade has been supported in part by the project with code RD/0121-MEITY01-001.

velocity. The phase difference at each element of a UPA allows us to estimate the Doppler frequency shift and velocity of the UAV's motion. We propose a novel scheme based on relative phase and projection matrix computation. The projection matrix in a UPA shapes the spatial response of the array. This steers the beam towards the desired directions and achieves optimal beam-steering characteristics. Our proposed scheme offers better statistical performance than those in prior work since it can be applied to both linear and non-linear channel models and can provide a uniform framework for estimation. Using extensive numerical computations, we show that our proposed scheme computes estimates of the channel, Doppler frequency shift, as well as UAV velocity that are highly accurate; also, the mean errors of the estimates of the Doppler frequency shift computed by our proposed scheme are much closer to zero than those of the estimates computed using the state-of-the-art chirplet transform based algorithm [7].

The rest of this paper is organized as follows. Section II provides a review of related work. Sections III and IV describe the system model and problem formulation, respectively. Section V presents a beam-steering procedure to model the UAV in the beam-space. Section VI describes the proposed scheme for UAV channel, Doppler frequency shift, and velocity estimation. Section VII presents numerical results and Section VIII provides conclusions and directions for future research.

II. Related Work

Most of the existing works on Doppler frequency shift and velocity estimation assume that channel state information (CSI) is available. In several of them, e.g., [8]–[12], multiple-input multiple-output (MIMO) antenna based approaches have been extensively explored. Note that the phased array-based UAV system discussed in [12] is different from the conventional MIMO architecture. The most important difference is that incremental changes in phase are deployed across different antenna elements instead of applying the same phase across all the elements [12]. This results in a beam pattern that depends on the velocity, angle, and orientation of the UAV. Doppler frequency shift estimation in phased array systems typically involves determining the direction cosines of the signals emitted from the UAV. The goal is to accurately estimate the channel response to enable efficient data transmission and reception by spatial filtering. However, the above works [8]–[12] do not address the problem of estimation of the channel between the UAV and the GS.

In [6], position and channel estimation schemes for UAV communication are proposed, which may not be effective in non-linear channel models, especially when dealing with complex relationships between parameters such as the channel and position. In [13], a MLE based technique for computing the position estimate is proposed. However, the work in [13] is limited only to static objects. A scheme for Doppler frequency shift estimation using the chirplet transform is proposed in [7]. However, in Section VII, we show using simulations that the mean errors of the estimates of the Doppler frequency shift computed by our proposed scheme are much closer to zero than those of the estimates computed using the scheme proposed in [7].

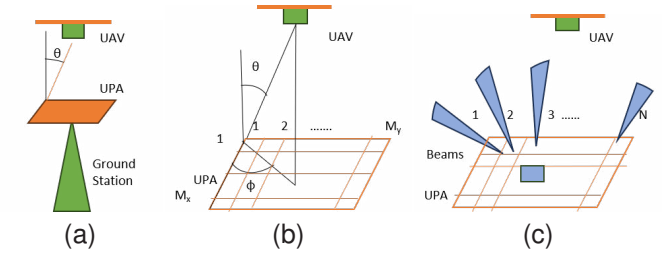

Fig. 1. Fig. (a) shows the UAV and the GS. Fig. (b) shows the $M_x \times M_y$ UPA at the GS. Fig. (c) shows the N beams formed by the UPA.

III. System Model

We consider a scenario consisting of a UAV communicating with a GS using mmWave technology as shown in Fig. 1a. The GS is equipped with a $M_x \times M_y$ UPA, and the UAV is equipped with a single antenna as illustrated in Fig. 1b. Multiple antenna elements are used at the GS since they improve the capacity and reliability of communication. The total number of antenna elements at the GS is $M = M_x M_y$. The traveling velocity of the UAV towards the GS and the channel gain factor between the UAV and the GS are denoted by v_d and α, respectively. The UAV is moving at a constant altitude in a horizontal plane, which is parallel to the UPA. The traveling velocities of the UAV towards different elements of the UPA are assumed to be the same, since their angles of arrival are nearly the same, due to the far-field effect [14].

IV. Problem Formulation

Suppose the received radio signal frequency at the m^{th} antenna element of the GS is defined as f_m and is observed for a time duration T. The complex envelope of the received signal, $y_m(t)$, at the m^{th} antenna array element of the GS at time instant t is modeled as:

$$y_m(t) = \psi(t - \tilde{\tau}_m)\,\alpha e^{-j2\pi \tilde{f}_m t} + \rho_m(t) \quad \text{for } m \in \{0, 1, \ldots, M-1\},\ 0 \le t \le T, \quad (1)$$

where $\psi(t)$ and $\tilde{\tau}_m$ are the transmitted signal and the delay in the signal propagation from the UAV to the m^{th} antenna array element of the GS, respectively. Further, $\rho_m(t)$ is additive white Gaussian noise with zero mean and variance σ^2. As shown in Fig. 1b, the signal is received from a direction (θ, ϕ), where θ and ϕ denote the polar and the azimuthal angles, respectively, in the spherical coordinate system. The initial values of θ and ϕ are known to the GS. Recall that the UAV is moving parallel to the UPA; also, the coordinate system is such that ϕ remains constant when the UAV moves. Furthermore, $\tilde{\tau}_m$ is given by (see Fig. 1b):

$$\tilde{\tau}_m = \frac{c_{x,m} d_x \sin\theta \cos\phi + c_{y,m} d_y \sin\theta \sin\phi}{c}, \quad (2)$$

where $c_{x,m}$ and $c_{y,m}$ are the indices of the m^{th} element in the x and y directions, respectively, and d_x and d_y are the separation between the nearest array elements in the x and y directions, respectively. Further, c is the radio frequency (RF) signal's speed of propagation in air.

Next, we employ direction cosines to describe the orientations of vectors without relying on a particular set of

coordinates in space. Let the direction cosines u and v be defined as: $u = \sin\theta\cos\phi$ and $v = \sin\theta\sin\phi$, respectively; then (2) yields:

$$\tilde{\tau}_m = \frac{c_{x,m}d_x u + c_{y,m}d_y v}{c}. \tag{3}$$

Due to the narrow-band approximation, the time delay $\tilde{\tau}_m$ is very small compared to the characteristic period T_s of the signal [14], i.e.:

$$\tilde{\tau}_m << T_s.$$

Note that the signal used for UAV navigation and positioning can be assumed to be narrow-band since its bandwidth is small compared to the coherent bandwidth of the channel. Therefore, all the frequency components of the signal experience nearly the same delay and phase shift. Hence, $\psi(t-\tilde{\tau}_m) \approx \psi(t)$. Therefore, (1) can be rewritten as:

$$y_m(t) \approx \psi(t)\,\alpha e^{-j2\pi\tilde{f}_m t} + \rho_m(t). \tag{4}$$

The problem is as follows: given the output $y_m(\cdot)$ at the m^{th} element, $m \in \{0,1,\ldots,M-1\}$, estimate the channel between the UAV and the GS, the Doppler frequency shift, say f_d, and hence the UAV velocity v_d.

V. Beam-steering Procedure to Model UAV in Beam-space

When the UAV moves towards the GS with a nominal velocity v_d, the frequency of the signals received at the GS appears to increase, which is known as positive Doppler shift. In terms of f_c, the known transmitted signal carrier frequency, the Doppler shift in frequency, f_d, can be written as [13], [15]:

$$f_d = \frac{v_d \sin\theta f_c}{c}. \tag{5}$$

The received signal is sampled at times $t_q = q\Delta t$, where $q \in \{1,2,\ldots,Q\}$. Here, Q is the number of samples and $\Delta t = T/Q$. The signal at the t_q^{th} time sample is given by $y_m[q] = y_m(q\Delta t)$. The carrier frequency, $\tilde{f}_c$, observed by the m^{th} element at the t_q^{th} time sample is given by [15]:

$$\tilde{f}_c = f_c\frac{\tilde{\tau}_m}{t_q} = f_c\frac{\tilde{\tau}_m}{q\Delta t},\ m \in \{0,1,\ldots,M-1\}. \tag{6}$$

The observed signal frequency, $\tilde{f}_m$, at the m^{th} element can be written as [15]:

$$\tilde{f}_m = \tilde{f}_c(1+\mu_m), \tag{7}$$

where $\mu_m = \frac{v_d \sin\theta q\Delta t}{c_{x,m}d_x u + c_{y,m}d_y v}$. Using (3), (5), (6), and (7), the quantity $\tilde{f}_m t_q$ simplifies to:

$$\tilde{f}_m t_q = f_d t_q + \frac{(c_{x,m}d_x u + c_{y,m}d_y v)}{\lambda}, \tag{8}$$

where $\lambda = \frac{c}{f_c}$. Using (4) and (8), we can express $y_m(t_q), m \in \{0,1,\ldots,M-1\},\ q \in \{1,\ldots,Q\}$, as:

$$y_m(t_q) = \psi(t_q)\, e^{-j2\pi f_d t_q}\alpha e^{-j2\pi\frac{(c_{x,m}d_x u + c_{y,m}d_y v)}{\lambda}} + \rho_m(t_q). \tag{9}$$

Forming an array steering vector allows for the creation of a beam that is steered towards the current direction of the UAV. An array steering vector is essentially a set of weights applied to each element of the antenna array. By adjusting the phases of these weights, the relative phase differences between different elements can be tuned appropriately, leading to constructive interference in the desired direction and destructive interference in the other directions. This enhances the quality of the received signal. The $M \times 1$ output vector $\tilde{\mathbf{a}}(u,v)$ towards the u,v direction is given by [16]:

$$\tilde{\mathbf{a}}(u,v) = e^{-j\frac{2\pi}{\lambda}(c_{x,m}d_x u + c_{y,m}d_y v)}, m \in \{0,1,\ldots,M-1\}. \tag{10}$$

Fig. 1c shows the formation of N beams for the search of the UAV's position. Note that the number of beams is strictly less than the total number of antenna elements, i.e., $N < M$. The process of adjusting the coefficients of the complex exponentials in (10) by successively varying directional cosines yields different beams associated with the array elements.

We assume that there is no interference. Let the GS be located at the origin of a hypothetical sphere with radius r, which is the distance at which the power from the GS gets halved, i.e., reduced by 3 dB [17]. By adjusting the phase shifts assigned to each element, the overall array factor can be pointed in a particular direction u_n, v_n in space. The direction of the n^{th} beam is defined as [17]:

$$u_n = u_{3dB}\cos\delta_n,\ v_n = v_{3dB}\sin\delta_n,\ n \in \{0,\ldots,N-1\}, \tag{11}$$

where δ_n denotes a change in the beam pointing direction and can be written as $\delta_n = \frac{2\pi n}{N}$. Further, (u_{3dB}, v_{3dB}) denotes the 3 dB beamwidth. It is the point in the beam-space at which the power of antenna radiation reduces by half (i.e., changes by -3 dB). Equations (10) and (11) hold because adjusting the direction cosines in the array factor equation (10) allows the array to steer the main beam in the desired direction.

Now, the beam vector characterizes the spatial sensitivity of the array output in different directions. The $N \times 1$ beam vector $\tilde{\mathbf{b}}(u_n, v_n),\ n \in \{0,\ldots,N-1\}$, associated with the m^{th} element can be expressed as [13]:

$$\tilde{\mathbf{b}}(u_n, v_n) = \frac{1}{\sqrt{M}} e^{-j\frac{2\pi}{\lambda}(c_{x,m}d_x u_n + c_{y,m}d_y v_n)}. \tag{12}$$

The beam-steering process entails combining the individual signals received by the elements of the antenna array in a way that emphasizes signals transmitted towards a specific direction. It involves changing the pointing direction of the main lobe of the radiation pattern. We wish to form clutter-free beams towards the directions: $(u_1,v_1),(u_2,v_2),\ldots,(u_N,v_N)$.

Now, the beam-steering matrix typically refers to a mathematical object that describes how the main beam of a phased array antenna system can be electronically steered in different directions. The array steering vector is typically combined with the weights applied to the array elements to form the beam-steering matrix. The $N \times M$ beam-steering matrix $\tilde{\mathbf{A}}$ obtained by focusing the beam towards a point (u_p, v_p) is [17]:

$$\tilde{\mathbf{A}} = \tilde{\mathbf{b}}(u_n, v_n) \otimes \tilde{\mathbf{a}}(u_p, v_p)^T, \tag{13}$$

where $\otimes$ is the Kronecker product [18]. One can multiply the set of M output vectors $\tilde{\mathbf{a}}(u_p, v_p)$ from the array by the $N \times M$

beam-steering matrix $\tilde{\mathbf{A}}$. This multiplication yields directivity of the transmitted signal from the UPA in a desired direction. Taking into account the wireless fading effect, the $N \times 1$ beam vector, $\mathbf{a}$, which includes the beam-steering matrix $\tilde{\mathbf{A}}$, is given by:

$$\mathbf{a} = \alpha \tilde{\mathbf{A}} \tilde{\mathbf{a}}. \tag{14}$$

We can write the beam-space outputs, $y_n, \forall n \in \{1, \ldots, N\}$, as [15]:

$$\begin{aligned} y_1 &= \boldsymbol{\beta}_1 \boldsymbol{\psi}_1 a_1 + \rho_1, \\ y_2 &= \boldsymbol{\beta}_2 \boldsymbol{\psi}_2 a_2 + \rho_2, \\ &\vdots \\ y_N &= \boldsymbol{\beta}_N \boldsymbol{\psi}_N a_N + \rho_N, \end{aligned} \tag{15}$$

where $\boldsymbol{\beta}_n$ and $\boldsymbol{\psi}_n$ are $1 \times N$ and $N \times 1$ vectors, respectively. Further, a_n and ρ_n are scalars. That is, the $N \times 1$ output vector $\mathbf{y}$ in beam-space can be written as:

$$\mathbf{y} = \boldsymbol{\beta} \boldsymbol{\psi} \mathbf{a} + \boldsymbol{\rho}, \tag{16}$$

where $\boldsymbol{\psi}$ is the $N \times N$ transmitted signal matrix with full rank. The $N \times N$ diagonal matrix $\boldsymbol{\beta}$ is defined as:

$$\boldsymbol{\beta} = diag\left[1, e^{-j2\pi f_d T_s}, \ldots, e^{-j2\pi f_d (N-1) T_s}\right], \tag{17}$$

where the '$diag$' operator denotes a diagonal matrix with its principal diagonal entries specified in the arguments of the operator. The $N \times 1$ noise vector $\boldsymbol{\rho}$ is zero mean with covariance matrix $\mathbf{C}$. The $N \times 1$ desired beam-space data vector is $\tilde{\mathbf{y}} = \boldsymbol{\beta} \boldsymbol{\psi} \mathbf{a}$. After beams have been produced, further processing is performed on the beams. We explain the estimation of the desired UAV parameters based on MLE in the next section.

VI. UAV's Channel, Doppler Shift, and Velocity Estimation

In this section, we explain how the channel, Doppler shift, and velocity for the communication between the UAV and the GS can be estimated. The proposed estimation technique uses the MLE algorithm.

The probability density function (PDF) $p(\boldsymbol{\rho})$ of $\boldsymbol{\rho}$ is given by [19]:

$$p(\boldsymbol{\rho}) = \frac{1}{(2\pi)^{N/2} (\det(\mathbf{C}))^{1/2}} e^{\left(-\frac{1}{2} \boldsymbol{\rho}^H \mathbf{C}^{-1} \boldsymbol{\rho}\right)},$$

where $\mathbf{C}$ is a $N \times N$ noise covariance matrix defined as $\mathbf{C} = \sigma^2 \mathbf{I}$, $\mathbf{I}$ is the $N \times N$ identity matrix, and w^H denotes the Hermitian operator on matrix w. Thus, the PDF of observing $\mathbf{y}$ under specific values of $\mathbf{a}$ and $\boldsymbol{\beta}$ is given by:

$$p(\mathbf{y}|\mathbf{a}, \boldsymbol{\beta}) = \frac{1}{\sigma (2\pi)^{N/2}} e^{-\frac{\|\mathbf{y} - \boldsymbol{\beta}\boldsymbol{\psi}\mathbf{a}\|^2}{2\sigma^2}}. \tag{18}$$

Therefore, the joint maximum likelihood estimates of $\mathbf{a}$ in (14) and f_d in (5), denoted by $\hat{\mathbf{a}}$ and $\hat{f}_d$, respectively, are given as follows:

$$\left[\hat{\mathbf{a}} \ \hat{f}_d\right] = \underset{\mathbf{a} \ f_d}{\operatorname{argmax}} \ p(\mathbf{y}|\mathbf{a}, \boldsymbol{\beta}).$$

By (18), this is equivalent to the following:

$$[\hat{\mathbf{a}} \ \hat{f}_d] = \underset{\mathbf{a} \ f_d}{\operatorname{argmin}} \ \|\mathbf{y} - \boldsymbol{\beta}\boldsymbol{\psi}\mathbf{a}\|^2. \tag{19}$$

The estimate $\hat{\mathbf{a}}$ can be obtained by finding the gradient of $\|\mathbf{y} - \boldsymbol{\beta}\boldsymbol{\psi}\mathbf{a}\|^2$ and equating it to zero; this yields:

$$\hat{\mathbf{a}} = \left(\boldsymbol{\psi}^H \boldsymbol{\psi}\right)^{-1} \boldsymbol{\psi}^H \boldsymbol{\beta}^H \mathbf{y}. \tag{20}$$

Using (19) and (20), $\hat{f}_d$ can be written as:

$$\hat{f}_d = \underset{f_d}{\operatorname{argmin}} \ \|\mathbf{y} - \boldsymbol{\beta}\mathcal{P}_s\boldsymbol{\beta}^H\mathbf{y}\|^2, \tag{21}$$

where $\mathcal{P}_s$ is a projection matrix and is given by:

$$\mathcal{P}_s = \boldsymbol{\psi}\left(\boldsymbol{\psi}^H \boldsymbol{\psi}\right)^{-1} \boldsymbol{\psi}^H. \tag{22}$$

A projection matrix plays a crucial role in estimation by spatial signal processing [5]. The projection matrix is used to project the received signals from the antenna array elements onto a specific abstract subspace. This subspace corresponds to the desired direction or steering angle. This filters out components of the received signals that are not aligned with the desired direction, providing spatial selectivity.

Since $\boldsymbol{\beta}^H\boldsymbol{\beta} = I$, and by (17) and the idempotent property of $\mathcal{P}_s$, the expression in (21) can be further simplified as follows:

$$\|\mathbf{y} - \boldsymbol{\beta}\mathcal{P}_s\boldsymbol{\beta}^H\mathbf{y}\|^2 = \mathbf{y}^H\mathbf{y} - \mathbf{y}^H\boldsymbol{\beta}\mathcal{P}_s\boldsymbol{\beta}^H\mathbf{y}.$$

So (21) is equivalent to:

$$\begin{aligned} \hat{f}_d &= \underset{f_d}{\operatorname{argmax}} \ \mathbf{y}^H\boldsymbol{\beta}\mathcal{P}_s\boldsymbol{\beta}^H\mathbf{y} \\ &= \underset{f_d}{\operatorname{argmax}} \ f(f_d), \end{aligned} \tag{23}$$

where $f(f_d)$ is given by:

$$f(f_d) = \mathbf{y}^H\boldsymbol{\beta}\mathcal{P}_s\boldsymbol{\beta}^H\mathbf{y}. \tag{24}$$

In order to maximize $f(f_d)$, we take the partial derivative of $f(f_d)$ with respect to f_d and equate it to zero as follows:

$$f'(f_d) = \frac{\partial f(f_d)}{\partial f_d} = 0.$$

Now, we use the Taylor series expansion for the first derivative, $f'(f_d)$, which is as follows:

$$f'(f_d) = f'(f_d)\big|_{f_d=\hat{f}_d} + f''(f_d)\big|_{f_d=\hat{f}_d}\Delta f_d + \ldots \tag{25}$$

Next, we derive expressions for $f'(f_d)$ and $f''(f_d)$, which appear in (25). Interestingly, by (17), the partial derivative of $\boldsymbol{\beta}$ with respect to f_d can be simplified as:

$$\begin{aligned} \frac{\partial\boldsymbol{\beta}}{\partial f_d} &= -j2\pi T_s \ diag\left[0, e^{-j2\pi f_d T_s}, \ldots, (N-1)e^{-j2\pi f_d (N-1) T_s}\right] \\ &= -j\mathbf{D}\boldsymbol{\beta}, \end{aligned} \tag{26}$$

where $\mathbf{D}$ is given by:

$$\mathbf{D} = 2\pi T_s \ diag\left[0, 1, \ldots, (N-1)\right]. \tag{27}$$

Further, taking a partial derivative of $\mathbf{y}$ given in (16), we can write:

$$\frac{\partial \mathbf{y}}{\partial f_d} = -j\mathbf{D}\boldsymbol{\beta}\boldsymbol{\psi}\mathbf{a}. \tag{28}$$

Similarly, $\frac{\partial \boldsymbol{\beta}^H}{\partial f_d}$ can be easily obtained as $\frac{\partial \boldsymbol{\beta}^H}{\partial f_d} = j\boldsymbol{\beta}^H\mathbf{D}$. By the chain rule, (24), (26), and (28), the partial derivative of $f(f_d)$ with respect to f_d is given by:

$$\begin{aligned} f'(f_d) &= 2\mathbf{y}^H\boldsymbol{\beta}\mathcal{P}_s\left(\boldsymbol{\beta}^H\frac{\partial \mathbf{y}}{\partial f_d} + \frac{\partial \boldsymbol{\beta}^H}{\partial f_d}y\right) \\ &= 2j\mathbf{y}^H\boldsymbol{\beta}\mathcal{P}_s\boldsymbol{\beta}^H\mathbf{D}\boldsymbol{\rho}. \end{aligned} \tag{29}$$

Now, recall that $\mathbf{y}$ is the sum of the desired signal, $\tilde{\mathbf{y}}$, and the additive white Gaussian noise vector, $\boldsymbol{\rho}$, i.e.:

$$\mathbf{y} = \tilde{\mathbf{y}} + \boldsymbol{\rho}. \tag{30}$$

Using (30), (29) can be written as:

$$\begin{aligned} f'(f_d) &= 2j\left(\tilde{\mathbf{y}}^H + \boldsymbol{\rho}^H\right)\boldsymbol{\beta}\mathcal{P}_s\boldsymbol{\beta}^H\mathbf{D}\boldsymbol{\rho} \\ &= 2j\tilde{\mathbf{y}}^H\boldsymbol{\beta}\mathcal{P}_s\boldsymbol{\beta}^H\mathbf{D}\boldsymbol{\rho} + 2j\boldsymbol{\rho}^H\boldsymbol{\beta}\mathcal{P}_s\boldsymbol{\beta}^H\mathbf{D}\boldsymbol{\rho}. \end{aligned} \tag{31}$$

The vector $\mathbf{D}\boldsymbol{\rho}$ in the noise subspace is orthogonal to the vector $\boldsymbol{\beta}^H\mathcal{P}_s\boldsymbol{\beta}\tilde{\mathbf{y}}$ in the signal subspace [19]. Hence, the first term in (31) is zero. This yields the following expression:

$$\begin{aligned} f'(f_d) &= 2j\boldsymbol{\rho}^H\boldsymbol{\beta}\mathcal{P}_s\boldsymbol{\beta}^H\mathbf{D}\boldsymbol{\rho} \\ &= \mathit{Img}\{-2\boldsymbol{\rho}^H\boldsymbol{\beta}\mathcal{P}_s\boldsymbol{\beta}^H\mathbf{D}\boldsymbol{\rho}\}, \end{aligned} \tag{32}$$

where $\mathit{Img}\{z\}$ denotes the imaginary part of z.

The relative velocity of the UAV with respect to the GS may have a distribution over multiple velocities due to small deviations from a fixed deterministic value. This is because of deviations from a fixed aerodynamic scenario. Hence, we take expectation over all possible scenarios. Taking expectations on both sides of (32) and simplifying, we get the following:

$$\mathrm{E}\{f'(f_d)\} = j2\sigma^2\,\mathrm{Tr}[\boldsymbol{\beta}\mathcal{P}_s\boldsymbol{\beta}^H\mathbf{D}], \tag{33}$$

where Tr denotes the trace operator. Using (26), the second derivative of (32) is given by:

$$\begin{aligned} f''(f_d) &= 2j\boldsymbol{\rho}^H\frac{\partial \boldsymbol{\beta}}{\partial f_d}\mathcal{P}_s\boldsymbol{\beta}^H\mathbf{D}\boldsymbol{\rho} + 2j\boldsymbol{\rho}^H\boldsymbol{\beta}\mathcal{P}_s\frac{\partial \boldsymbol{\beta}^H}{\partial f_d}\mathbf{D}\boldsymbol{\rho} \\ &= 2\boldsymbol{\rho}^H\mathbf{D}\boldsymbol{\beta}\mathcal{P}_s\boldsymbol{\beta}^H\mathbf{D}\boldsymbol{\rho} - 2\boldsymbol{\rho}^H\boldsymbol{\beta}\mathcal{P}_s\boldsymbol{\beta}^H\mathbf{D}^2\boldsymbol{\rho}. \end{aligned} \tag{34}$$

Similar to (33), we can write the following:

$$\begin{aligned} \mathrm{E}\{f''(f_d)\} &= \mathrm{E}\{2\boldsymbol{\rho}^H\mathbf{D}\boldsymbol{\beta}\mathcal{P}_s\boldsymbol{\beta}^H\mathbf{D}\boldsymbol{\rho} - 2\boldsymbol{\rho}^H\boldsymbol{\beta}\mathcal{P}_s\boldsymbol{\beta}^H\mathbf{D}^2\boldsymbol{\rho}\} \\ &= 2\sigma^2\,\mathrm{Tr}[\mathbf{D}\boldsymbol{\beta}\mathcal{P}_s\boldsymbol{\beta}^H\mathbf{D}] - 2\sigma^2\,\mathrm{Tr}[\boldsymbol{\beta}\mathcal{P}_s\boldsymbol{\beta}^H\mathbf{D}^2]. \end{aligned} \tag{35}$$

By (23), the first derivative of $f(f_d)$ is equal to zero at $\hat{f}_d$ because it is a stationary point [19]. Using this fact, neglecting the higher derivative terms in the series in (25), and using (31) and (34), the change in Doppler shift, Δf_d, can be expressed as follows:

$$\begin{aligned} \Delta f_d &= -\frac{\mathrm{E}\{f'(f_d)\big|_{f_d=\hat{f}_d}\}}{\mathrm{E}\{f''(f_d)\big|_{f_d=\hat{f}_d}\}} \\ &= -\frac{\mathit{Img}\{\mathrm{Tr}[\boldsymbol{\beta}\mathcal{P}_s\boldsymbol{\beta}^H\mathbf{D}]\}}{\left(\mathrm{Tr}[\mathbf{D}\boldsymbol{\beta}\mathcal{P}_s\boldsymbol{\beta}^H\mathbf{D}] - \mathrm{Tr}[\boldsymbol{\beta}\mathcal{P}_s\boldsymbol{\beta}^H\mathbf{D}^2]\right)}. \end{aligned} \tag{36}$$

TABLE I
THE TABLE SHOWS THE VALUES OF THE PARAMETERS USED FOR OUR SIMULATIONS.

Parameter	Value
M_x, M_y, N	2
f_c	28×10^9 Hz
c	3×10^8 m/s
R	5 m
α	0.5
T_s	1.1 sec

Therefore, our estimate of the Doppler frequency, $\hat{f}_d$, can be obtained as follows [15]. By the aid of (5), the Doppler frequency f_d is obtained assuming that the initial UAV velocity, v_d, is known. The received signal frequency deviates from that of the transmitted signal due to Doppler shift [1]. This perturbation leads to a complex Doppler frequency estimation process. To simplify this, the Doppler frequency shift Δf_d is required. The estimate $\hat{f}_d$ differs from the Doppler frequency f_d by the change in Doppler shift Δf_d. Thus, by (36):

$$\begin{aligned} \hat{f}_d &= f_d + \Delta f_d \\ &= f_d + \frac{\mathit{Img}\{\mathrm{Tr}[\boldsymbol{\beta}\mathcal{P}_s\boldsymbol{\beta}^H\mathbf{D}]\}}{\left(\mathrm{Tr}[\boldsymbol{\beta}\mathcal{P}_s\boldsymbol{\beta}^H\mathbf{D}^2] - \mathrm{Tr}[\mathbf{D}\boldsymbol{\beta}\mathcal{P}_s\boldsymbol{\beta}^H\mathbf{D}]\right)}. \end{aligned} \tag{37}$$

Using the Doppler shift, we can obtain the following estimate of the UAV velocity, $\hat{v}_{UAV}$, [15]:

$$\hat{v}_{UAV} = \frac{\lambda}{\sin\theta}\left(f_d + \Delta f_d\right), \tag{38}$$

where Δf_d is given by (36).

In summary, with the prior knowledge of the transmitted signal and using MLE, we can estimate the channel using (20) as well as the Doppler shift using (37). Also, the estimated Doppler shift can then be used to estimate the UAV velocity using (38).

VII. Numerical Results

In this section, we evaluate the performance of our channel, Doppler frequency shift, and UAV velocity estimation scheme using MATLAB simulations. In our simulations, the UAV's nominal velocity is 30 m/s and it travels towards the GS at a constant altitude. Initially, the azimuthal and elevation angles made by the UAV with respect to the GS are 20° and 10°, respectively. Table I specifies the remaining parameters used for our simulations. After every 0.1 ms, we estimate the channel, Doppler frequency shift, as well as the UAV velocity. A digital pulse with duty cycle $20\,\%$ is modulated using Phase Shift Keying (PSK) modulation and treated as the transmitted signal. The received signal is observed with different Signal-to-Noise Ratios (SNRs) varying from 0 to 10 dB. With an adequate sampling frequency, 1000 samples are considered to estimate the channel, Doppler frequency shift, and hence the UAV velocity, over 50 iterations.

Fig. 2a shows a comparison of the actual Doppler frequency shift and the estimated Doppler frequency shift. Fig 2b shows a comparison of the actual UAV relative velocity and the estimated relative velocity. It can be seen from Fig. 2 that the estimates computed by our proposed scheme are very close

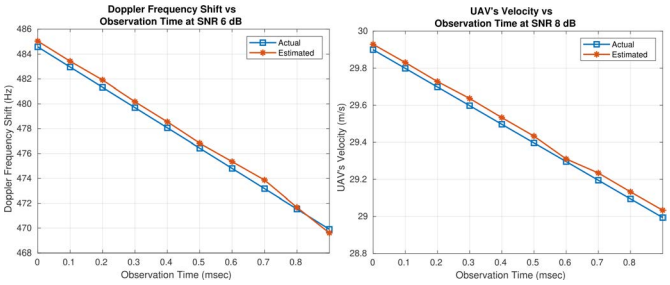

Fig. 2. Fig. (a) shows a comparison of the actual and estimated Doppler frequency shifts at an SNR of 6 dB. Fig. (b) shows a comparison of the actual and estimated velocities of the UAV at an SNR of 8 dB.

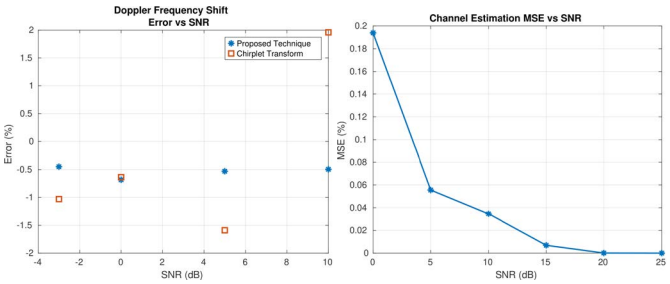

Fig. 3. Fig. (a) shows a comparison of the mean errors of the estimates of the Doppler frequency shift computed by our proposed scheme and those of the estimates computed by the algorithm based on the chirplet transform [7] for the SNR values -3, 0, 5 and 10 dB. Fig. (b) shows the MSEs of the estimates of the channel information computed by our proposed scheme for different values of the SNR.

to the actual Doppler frequency shifts and UAV velocities. Next, Fig. 3a shows a comparison of the mean errors in the estimation of the Doppler frequency shift under our proposed scheme and under the algorithm based on the chirplet transform proposed in [7]. It can be clearly seen from the figure that the mean errors of the estimates computed by our proposed scheme are much closer to zero than those of the estimates computed using the chirplet transform based algorithm [7]. Fig. 3b shows the mean squared errors (MSE) of the estimates of channel information computed by our proposed scheme at different SNRs varying from 0 dB to 25 dB with increments of 5 dB. As expected, the MSEs decrease in the SNR; also, the figure shows that the MSEs are very small for all the values of SNRs used. In summary, our numerical results show that our proposed scheme computes highly accurate estimates of the channel, Doppler frequency shift, as well as UAV velocity; also, the mean errors of the estimates of the Doppler frequency shift computed by our proposed scheme are much closer to zero than those of the estimates computed using the state-of-the-art chirplet transform based algorithm [7].

VIII. Conclusions and Future Work

We proposed an improved scheme for estimating the UAV channel, Doppler frequency shift, and velocity, when it communicates with a GS using antenna arrays and mmWave frequency bands. Using extensive numerical results, we showed that our proposed scheme computes estimates of the channel, Doppler frequency shift, as well as UAV velocity that are highly accurate; also, the mean errors of the estimates of the Doppler frequency shift computed by our proposed scheme are much closer to zero than those of the estimates computed using the state-of-the-art chirplet transform based algorithm [7]. A direction for future research is to analytically derive upper bounds on the estimation errors under our proposed scheme.

References

[1] Y. Zeng, Q. Wu, and R. Zhang, "Accessing from the sky: A tutorial on UAV communications for 5G and beyond," *Proceedings of the IEEE*, vol. 107, no. 12, pp. 2327–2375, 2019.

[2] M. Mozaffari, W. Saad, M. Bennis, Y.-H. Nam, and M. Debbah, "A tutorial on UAVs for wireless networks: Applications, challenges, and open problems," *IEEE Communications Surveys & Tutorials*, vol. 21, no. 3, pp. 2334–2360, 2019.

[3] A. Agrahari, P. Varshney, and A. K. Jagannatham, "Precoding and downlink beamforming in multiuser MIMO-OFDM cognitive radio systems with spatial interference constraints," *IEEE Transactions on Vehicular Technology*, vol. 67, no. 3, pp. 2289–2300, 2017.

[4] M. Mozaffari, W. Saad, M. Bennis, and M. Debbah, "Communications and control for wireless drone-based antenna array," *IEEE Transactions on Communications*, vol. 67, no. 1, pp. 820–834, 2018.

[5] D. Tse and P. Viswanath, *Fundamentals of wireless communication*. Cambridge University Press, 2005.

[6] H. Kwon and I. Guvenc, "RF signal source search and localization using an autonomous UAV with predefined waypoints," *arXiv preprint arXiv:2301.07027*, 2023.

[7] G. Yang, B. Xing, and Y. Dong, "High precision doppler estimation method for LFM signals based on Chirplet Transform," in *2022 IEEE 5th Advanced Information Management, Communicates, Electronic and Automation Control Conference (IMCEC)*, vol. 5. IEEE, 2022, pp. 1089–1092.

[8] P. Antonik, M. C. Wicks, H. D. Griffiths, and C. J. Baker, "Range-dependent beamforming using element level waveform diversity," in *2006 International Waveform Diversity & Design Conference*. IEEE, 2006, pp. 1–6.

[9] J. Chen, B. Daneshrad, and W. Zhu, "MIMO performance evaluation for airborne wireless communication systems," in *2011-MILCOM 2011 Military Communications Conference*. IEEE, 2011, pp. 1827–1832.

[10] D. Rieth, C. Heller, D. Blaschke, and G. Ascheid, "On the practicability of airborne MIMO communication," in *2015 IEEE/AIAA 34th Digital Avionics Systems Conference (DASC)*. IEEE, 2015, pp. 2C1–1.

[11] T. J. Willink, C. C. Squires, G. W. Colman, and M. T. Muccio, "Measurement and characterization of low-altitude air-to-ground MIMO channels," *IEEE Transactions on Vehicular Technology*, vol. 65, no. 4, pp. 2637–2648, 2015.

[12] E. Yanmaz, R. Kuschnig, and C. Bettstetter, "Achieving air-ground communications in 802.11 networks with three-dimensional aerial mobility," in *2013 Proceedings IEEE INFOCOM*. IEEE, 2013, pp. 120–124.

[13] W.-Q. Wang, "Range-angle dependent transmit beampattern synthesis for linear frequency diverse arrays," *IEEE Transactions on Antennas and Propagation*, vol. 61, no. 8, pp. 4073–4081, 2013.

[14] A. Goldsmith, "Capacity limits of MIMO channels," *IEEE Trans. Inf. Theory*, vol. 48, no. 6, pp. 1277–1294, 2000.

[15] A. J. Weiss and A. Amar, "Direct geolocation of stationary wideband radio signal based on time delays and Doppler shifts," in *2009 IEEE/SP 15th Workshop on Statistical Signal Processing*. IEEE, 2009, pp. 101–104.

[16] C. A. Balanis, *Antenna theory: analysis and design*. John Wiley & Sons, 2016.

[17] R. J. Mailloux, *Phased array antenna handbook*. Artech House, 2017.

[18] C. F. Van Loan, "The ubiquitous Kronecker product," *Journal of Computational and Applied Mathematics*, vol. 123, no. 1-2, pp. 85–100, 2000.

[19] S. P. Boyd and L. Vandenberghe, *Convex optimization*. Cambridge University Press, 2004.